Publications of the Astronomical Society of Australia (PASA), Vol. 34, e012, 7 pages (2017).

doi:10.1017/pasa.2017.6

Superluminous Supernovae at High Redshift

Tim Abbott[1], Jeff Cooke[2,3], Chris Curtin[2,3], Shahab Joudaki[2,3], Antonios Katsianis[4], Anton Koekemoer[5], Jeremy Mould[2,3,9], Edoardo Tescari[3,6], Syed Uddin[2,7] and Lifan Wang[8]

[1]Cerro Tololo Interamerican Observatory, Casilla 603, La Serena, Chile
[2]Centre for Astrophysics & Supercomputing, Swinburne University P.O. Box 318, Hawthorn, Victoria 3122, Australia
[3]ARC Centre of Excellence for All-sky Astrophysics (CAASTRO)
[4]Dept of Astronomy, Universidad de Chile, Camino El Observatorio 1515, Las Condes, Santiago, Chile
[5]Space Telescope Science Institute, 3700 San Martin Drive, Baltimore, MD21218, USA
[6]School of Physics, University of Melbourne, Swanston St & Tin Alley, Parkville Victoria 3010, Australia
[7]Purple Mountain Observatory, Chinese Academy of Sciences, Tianwentai Rd, Xuanwu Qu, Nanjing Shi, Jiangsu Sheng, China
[8]Texas A&M University, 400 Bizzell St, College Station, TX 77843, USA
[9]Email: jmould@swin.edu.au

(Received April 1, 2016; Accepted January 31, 2017)

Abstract

Superluminous supernovae are beginning to be discovered at redshifts as early as the epoch of reionisation. A number of candidate mechanisms is reviewed, together with the discovery programmes.

Keywords: dark ages, reionization, first stars – galaxies: high-redshift – stars: luminosity function, mass function – supernovae: general

1 INTRODUCTION

An unavoidable problem in probing the high-redshift Universe is the rapid rise of luminosity distance with redshift. In luminosity distance, the epoch of reionisation (EoR) from $t = 100$ Myrs extends 80 Hubble radii. More powerful telescopes and instruments are needed for the EoR, such as (i) *JWST*: [powerful, but small field, with spectroscopy paramount], (ii) DECam: [1 μm and shorter, wide field (Flaugher et al. 2012)], (iii) KDUST: [1 μm $< \lambda <$ 3 μm, wide field (Yuan et al. 2013)], (iv) Subaru: [Hyper Suprime Cam (HSC—Miyazaki 2015)]. In this paper, we review survey successes and expectations for superluminous supernovae (SLSNe).

2 MASSIVE AND SUPERMASSIVE STARS

We observe very massive stars (>100 $M_\odot$) in the present universe and, as a result, we do know that they can form. But how do they actually end their lives? Will they die as core-collapse supernovae (SNe) energised by the spin down of magnetars, pair instability supernovae (PISNe) with explosion energies up to 100 times that of regular SNe, pulsational PISNe that can produce very bright events due to colliding shells, or via another mechanism? Asymmetry may play a critical role in evolution. Extreme events that trigger relativistic jets may become luminous enough such that their discovery can be made by relatively small telescopes. These extreme cases may output high energy radiation as in gamma-ray bursts (GRB).

Woosley & Heger (2015) reviewed the theory of the evolution and death of stars heavier than 10 $M_\odot$ on the main sequence. The more massive of these, absent serious mass loss, either make black holes when they die, or, for helium cores exceeding ~35 $M_\odot$, encounter the pair instability. Outcomes, including the appearance of GRBs (Levan et al. 2016), depend on the initial composition of the star, its rotation rate, and detailed physics. These stars can produce some of the brightest SNe, but also some of the faintest.

Yoshida et al. (2014) investigated very massive stars with main sequence mass larger than 100 $M_\odot$ and metallicity 0.001 $< Z <$ 0.004 which might explode as Type Ic SLSNe. Progenitors of 43 and 61 $M_\odot$ WO stars with $Z = 0.004$ were evolved from initial 110 and 250 $M_\odot$ stars. These stars were expected to explode as Type le SNe. Other progenitor spectral types were studied by Groh et al. (2013). Dessart et al. (2012) point out that mixing challenges the ability to infer progenitor and explosion properties.

From the collapse of supermassive stars (SMSs), supermassive black holes observed at high redshift in QSOs could grow from direct collapse black holes (DCBHs) with mass $\sim 10^5$ $M_\odot$. Ultra-luminous SNe (Matsumoto et al. 2016) of $\sim 10^{45-46}$ erg s^{-1} would be detectable by future telescopes in the near infrared, such as Euclid, *WFIRST*, KDUST, and *JWST* for ∼5 000 d to $Z \lesssim 20$ and ∼100 events per year.

The unknowns in binary massive star evolution have recently received widespread attention with the detection of a massive binary inspiral (Abbott et al. 2016a). Understanding such events in the low-redshift Universe will enable us to better interpret high-redshift observations.

3 HIGH Z SNE

Does the collapse of pristine gas in the early Universe lead to the formation of very massive stars? Larson (1998), Heger & Woosley (2002), O'Shea & Norman (2007, 2008) have considered the possibility and the notion of a different initial mass function (IMF) from today's. Wide-area, deep surveys are seeing a rare class of SLSNe, 10–100 times more luminous than typical SNe (Quimby et al. 2011; Gal-Yam 2012). However, only $\gtrsim$50 SLSNe have been detected at low Z (Nicholl et al. 2015, Smith et al. 2007; GYL 2009; Pastorello et al. 2010; Gezari et al. 2009). One of these events with slow fade was thought to be powered by the radiative decay of ^{56}Ni (Gal-Yam et al. 2009). A single event has been identified as the first detection of a third type of SN with a pair-instability supernova (PISN). As discussed above, SLSNe might to occur with higher rate at earlier times, due to the presence of pristine gas and a top-heavy IMF, which favours the creation of massive stars. Overall, according to Tescari et al. (2014) and Katsianis et al. (2015), an efficient feedback mechanism is needed to obtain the observed star-formation rate functions and stellar mass functions at high redshifts and SLSN maybe could play a major role.

Physical models of SLSNe include PISNe, magnetars, quark novae, radiatively shocked circumstellar matter, and jet-cocoon structures. The energy output may be as high as 10^{55-56} ergs, exceeding the main sequence radiated energy of 100 $M_\odot$ stars at 10^{54} ergs. Models involving more than one of the concepts outlined below have been considered by Tolstov et al. (2017), Gal-Yam (2016), and Gilmer et al. (2016).

3.1. The PISN concept

PISNe have been theorised since the 1960s (Rakavy & Shaviv 1967; Barkat, Rakavy, & Sack 1967) as the result of the deaths of stars with progenitor masses of 140–260 $M_\odot$ (Heger & Woosley 2002; Kasen, Woosley, & Heger 2011). Stars this massive generate conditions in their cores that enable efficient conversion of γ-ray photons into electron–positron pairs, followed by rapid conversion of pressure-supporting radiation into rest mass, violent contraction, and run-away thermonuclear explosion, obliterating the star (Kozyreva et al. 2017; Chatzopoulos et al. 2015).

A number of events are candidates for PISN, including SN2007bi (Gal-Yam et al. 2009). For example, Lunnan et al. (2016) discuss a number of 07bi-like PISN candidates, and they have rise photometry, one of the key discriminants. The two high redshift SLSNe of Cooke et al. (2012) are perhaps the most robust PISN candidates known, in particular, the redshift 2 event.

3.2. Magnetars, quark novae

Energy injection by a magnetar with a rapid rotation rate and magnetic field of 0.1–1 × 10^{14} G may supply excess luminosity. Chatzopoulos et al. (2016) argue that this requires fine-tuning and extreme parameters for the magnetar, as well as the assumption of efficient conversion of magnetar energy into radiation.

Ouyed et al. (2016) show that a quark nova (the explosive transition of a neutron star to a quark star) occurring a few days following the SN explosion of an oxygen Wolf–Rayet star can account for SLSNe, including extreme energetics and a double-peaked light-curve. The expanding remnant is used to harness the kinetic energy ($> 10^{52}$ ergs) of the ejecta.

3.3. Radiatively shocked circumstellar matter and jet-cocoon structures

Blinnikov (2016) reviews calculations, not only of the magnetar model and PISNe, but also models explaining SLSN events with the minimum energy budget, involving multiple ejections of mass in presupernova stars. The radiative shocks produced in collisions of those shells may provide the required power. This class of the models he refers to as 'interacting' SNe.

Matsumoto et al. (2016) consider supermassive black holes at high redshift growing from DCBHs with masses $\sim 10^5$ $M_\odot$, resulting from the collapse of SMSs. If a relativistic jet is launched from a DCBH, then it can break out of the collapsing SMS and produce a GRB. Although most GRB jets may miss our line of sight, they show that the energy injected from the jet into a cocoon is huge $\sim 10^{55-56}$ erg, so that the cocoon fireball is observed as an ultra-luminous supernova of $\sim 10^{45-46}$ erg s^{-1}.

4 OBSERVING HIGH-REDSHIFT SLSNE

Two SLSNe at $Z \sim 2$ have been observed: a slow evolving PISN event (Cooke et al. 2012) and another SLSN-I type event. Other surveys for high Z SLSNe include the 'All-Sky Automated Survey for Supernovae' (ASAS-SN; Brown & Warren-Son Holoien 2016), the Palomar Transient Factory (Perley et al. 2016), Subaru HSC surveys (Tanaka et al. 2016), and *GAIA* (Staley & Fender 2016). The SUperluminous Supernova Host galaxIES (SUSHIES) survey (Schulze et al. 2016) aims to provide constraints on the progenitors of SLSNe by understanding the relationship to their host galaxies. Appendix A reports on the DECam Deep Fields programme. Mould et al. (2017) report the discovery of a $Z \approx 6$ SLSN in the NSF field.

Table 1. Expected number of SLSNe deg^{-2}.

Redshift interval Z (1)	# (deg^{-2}) (2)	m-M-20 $-2.5\log(1+Z)$ (mag) (3)
(1.0, 1.5)	2	23.8
(1.5, 2.0)	2.5	24.5
(2.0, 2.5)	2.5	25.0
(2.5, 3.0)	2.5	25.4
(3.0, 3.5)	2.5	25.7
(3.5, 4.0)	2.5	25.9
(4.0, 4.5)	2.5	26.1

Table 2. Dropout bandpass vs. redshift.

$\lambda_{eff}/(1+Z)$	
100/(1+0)	100 nm
360/(1+2.6)	*u*
480/(1+3.8)	*g*
670/(1+5.7)	*r*
820/(1+7.2)	*i*

4.1. SLSN rates

The rate of core collapse SNe is proportional to the star-formation rate and affected by the IMF. Many studies have been made at $Z < 0.3$ (e.g., Bazin et al. 2009); few at higher *Z*. Most core collapse SNe are too faint, although luminous type IIn and SLSNe are an exception. SLSNe are extremely luminous in the UV (Brown 2016, Yan et al. 2016) , whereas type Ia are not. Therefore, objects are expected to be detectable at high *z*. Cooke et al. (2012) suggest that, at $Z\sim 2$–4, the SLSN rate is $\sim 4 \times 10^{-7}$ Mpc^{-3} yr^{-1}. This is $\lesssim 0.1\%$ of the total core collapse SN rate at $0.9 < Z < 1.3$ found by Dahlen et al. (2012). The *Z* dependence of the SLSN rate has been predicted by Tanaka et al. (2012). At this rate, the surface density of SLSNe is given in column (2) of Table 1. For DECam, these objects are quite faint by redshift 4 (see column 3), but not beyond reach.

5 OTHER DECAM RESULTS

5.1. GW150914

We observed the Prime Field (Table 2) 107 d after LIGO's first detection of a binary black hole inspiral (Abbott et al. 2016a). The error box for GW150914 includes the prime field. The brightest objects present after the event and not present in 2012, 2013 with colours that exclude flare stars have $Z \approx 17.5$ i.e., $M_Z \approx -20.5$ at the distance of the event. However, the binary black hole merger model predicts no electromagnetic counterpart for the event (Abbott et al. 2016b). A brightening of at least 7.5 mag was generally seen for these objects, which were most likely SNe.

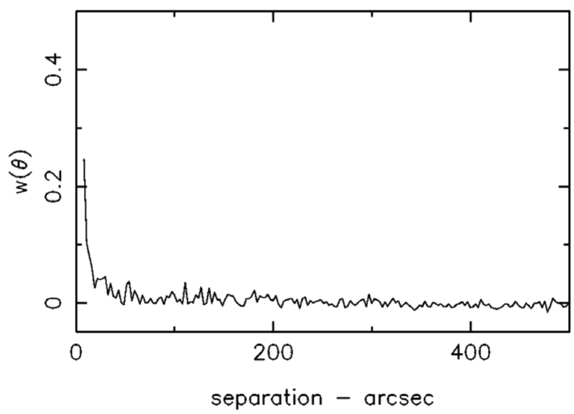

Figure 1. Angular correlation function for the NSF field. The scale at redshift 6 is 5.8 kpc arcsec^{-1}.

5.2. Large scale structure

Our first two nights of the DECamERON project yielded data on the prime field. Candidate *i* band dropouts have $Z \gtrsim 6$ and their structure across the 3 deg^2 field is far from uniform (Figure 1). Details are given by Mould (2013). The colour–magnitude diagram was shown by Mould (2015). Figure 1 is similar to that of Barone-Nugent et al. (2014). Reionisation lights up the gas on comoving scales of a few Mpc and more (Geil et al. 2016). This is accessible to the DECam Deep Field project.

5.3. Detection of SLSNe

Two of us (CC and JC) are working with SUDSS (Scovacricchi et al. 2016), using Lyman Break Galaxy (LBG) colour cuts for $Z = 3$. For present purposes, we modified these for higher redshift. The NSF field (Table 2) was drawn from SUDSS to increase the cadence. For $Z = 3.5$–4.8, these cuts are $g-r > r-i+0.8$; $g-i > 0.3$; $-0.7 < r-i < 1.2$; $-0.4 < i-z < 0.2$. These need further refinement. Figures A1–A3 (Appendix A) show our $Z = 4$ candidates. Mould et al. (2017) report the discovery of a $Z \approx 6$ SLSN in the NSF field based upon bandpass redshifts in Table 3.

6 HIGHER *Z* (TOWARDS THE DARK AGES)

There is absolutely no observational data on the stellar Universe at $z \sim 20$. Events at $z > 20$ need near infrared *K*-band observations. For this purpose, we can call on the low background and remarkable isoplanatism in Antarctica (Aristidi et al. 2013) to conduct wide field *K*-band time domain surveys. Spectroscopically, by the end of the decade, we shall have *JWST* to detect some of these SLSNe at redshifts all the way to $Z \sim 20$. While the explosion of first-generation stars is of fundamental importance, the rate of SLSNe at $Z \sim 20$ is highly uncertain and a low rate may limit the discovery space

Table 3. DECamERON programme (exposure times in kilosec).

Field	α, δ J2000		Exp time kilo s 2012 Dec 11	2013 Jan 12	2014 May 18	2015 Jul 23[a]	2016 Jan 1[b]
New Southern Field (NSF)		g				3.0	
		r				5.41	
	22:32:56	i			5.28	13.2	
	− 60:33	z			4.29	26.4	
		Y			14.85		
Prime field	5:55:07	g					2.0
	− 61:21	r					2.025
		i					1.65
		z	7.2	7.8			4.95
		Y	8.4	7.8			11.55
Polar field	16:00:00	r			2.5		
	− 75:00	i			9.9		
		z			18.48	7.5	
		Y			9.24	4.2	

[a]also 28/12
[b]also 8/8

of *JWST*. The deep NIR survey to $K = 29$th mag proposed by Wang[1] (2009) would be an excellent target feeder for *JWST*.

7 CONCLUSIONS

What we have seen in this brief review is a recent proliferation of SLSNe and a number of mechanisms that could be at work making them. The first 4 yrs of the DECamERON project suggest that DECam, like HSC, can penetrate the EoR. Large scale structure data are consistent with that of other programmes. There is every expectation that LBG and dropout selection criteria will allow EoR SLSNe to be found. Time dilation of high Z light curves allows economical observing. We plan to press on to investigate the fascinating scientific questions posed by the evolutionary end points of massive stars in the EoR. Among these are the possibility of using SLSNe for cosmology (Scovacricchi et al. 2016). The best route at higher Z may be to search for 'orphan' SLSNe that have the correct colours and then use very deep (*JWST*) spectroscopy to confirm the redshift.

ACKNOWLEDGEMENTS

We are grateful to the DES team for building DECam and the NVO at NOAO for flattening and stacking our data. Parts of this research were conducted by the Australian Research Council Centre of Excellence for All-sky Astrophysics (CAASTRO), through project number CE110001020. In addition to DAOPHOT, we used IRAF, a product of NOAO, which is operated by AURA and supported by NSF. Thanks also to our colleagues Stuart Wyithe, Chris Lidman, Michele Trenti, Robert Barone Nugent, and Andrea Kunder.

The DECamERON project used data obtained with the Dark Energy Camera, which was constructed by the Dark Energy Survey (DES) collaboration. Funding for the DES Projects has been provided by the DOE and NSF (USA), MISE (Spain), STFC (UK), HEFCE (UK). NCSA (UIUC), KICP (U. Chicago), CCAPP (Ohio State), MIFPA (Texas A&M), CNPQ, FAPERJ, FINEP (Brazil), MINECO (Spain), DFG (Germany), and the collaborating institutions in the Dark Energy Survey, which are Argonne Lab, UC Santa Cruz, University of Cambridge, CIEMAT-Madrid, University of Chicago, University College London, DES-Brazil Consortium, University of Edinburgh, ETH Zurich, Fermilab, University of Illinois, ICE (IEEC-CSIC), IFAE Barcelona, Lawrence Berkeley Lab, LMU Munchen and the associated Excellence Cluster Universe, University of Michigan, NOAO, University of Nottingham, Ohio State University, University of Pennsylvania, University of Portsmouth, SLAC National Lab, Stanford University, University of Sussex, and Texas A&M University.

REFERENCES

Abbott, B., et al. 2016a, PhRvL, 116, 1102
Abbott, B., et al. 2016b, ApJ, 826, L13
Aristidi, E., et al. 2013, IAU Symposium, 288, 300
Barone-Nugent, R., et al. 2014, ApJ, 793, 17
Barkat, Z., Rakavy, G., & Sack, N. 1967, PRL, 18, 379
Bazin, G., et al. 2009, A&A, 499, 653
Blinnikov, S. 2016, arxiv: 1611.00513
Brown, J., & Warren-Son Holoien, T. 2016, AAS, 227, 34913
Brown, P. 2016, AAS, 227, 23707
Chatzopoulos, E., et al. 2015, ApJ, 799, 18
Chatzopoulos, E., et al. 2016, ApJ, 828, 94
Cooke, J., et al. 2012, Nature, 491, 228
Dahlen, T., et al. 2012, ApJ, 757, 70
Dessart, L., et al. 2012, MNRAS, 424, 2139
Flaugher, B., et al. 2012, SPIE, 8446, 11
Gal-Yam, A. 2012, Science, 337, 927
Gal-Yam, A., & Leonard, D. 2009, Nature, 458, 865
Gal-Yam, A., et al. 2009, Nature, 462, 624
Gal-Yam, A. 2016, arxiv: 1611.09353
Geil, P., et al. 2016, MNRAS, 462, 804
Gezari, S., et al. 2009, ApJ, 690, 1313
Gilmer, M., et al. 2016, arxiv: 1610.00016
Groh, J., et al. 2013, A&A, 558, 131

[1] Z Equals Twenty from Antarctica (zETA) programme.

Heger, A., & Woosley, S. E. 2002, ApJ, 567, 532
Kasen, D., Woosley, S., & Heger, A. 2011, ApJ, 734, 102
Katsianis, A., et al. 2015, MNRAS, 448, 3001
Kozyreva, A., et al. 2017, MNRAS, 464, 2854
Larson, R. B. 1998, MNRAS, 301, 569
Levan, A., et al. 2016, SSRv, 202, 33
Lunnan, R., et al. 2016, ApJ, 831, 144
Matsumoto, T., et al. 2016, ApJ, 823, 83
Miyazaki, S. 2015, IAUGA, 225, 5916
Moriya, T., et al. 2016, ApJ, 833, 64
Mould, J. 2013, http://www.caastro.org/reionization-in-the-red-centre-presentations
Mould, J. 2015, ASP Conf. Ser., 491, 215
Mould, J., et al. 2017, submitted to Chinese Science Bulletin
Nicholl, M., et al. 2015, MNRAS, 452, 3869
O'Shea, B., & Norman, M. 2007, ApJ, 654, 66
O'Shea, B., & Norman, M. 2008, ApJ, 648, 31
Ouyed, R., et al. 2016, ApJ, in press, arxiv: 1611.03657
Pastorello, A., et al. 2010, ApJ, 724, 16
Perley, D., et al. 2016, ApJ, 830, 13
Quimby, R., et al. 2011, Nature, 474, 487
Rakavy, G., & Shaviv, G. 1967, ApJ, 148, 803
Scovacricchi, D., et al. 2016, MNRAS, 456, 1700
Smith, N., et al. 2007, ApJ, 666, 1116
Staley, T., & Fender, R. 2016, arXiv: 1606.03735
Tanaka, M., et al. 2012, MNRAS, 422, 2675
Tanaka, M., et al. 2016, ApJ, 819, 5
Tescari, E., et al. 2014, MNRAS, 438, 3490
Tolstov, A., et al. 2017, ApJ, 835, 266
Trenti, M., et al. 2010, ApJ, 714, 202
Valdes, F., et al. 2014, ASP Conf. Ser., 485, 379
Wang, L. 2009, AAS, 213, 22604
Woosley, S., & Heger, A. 2015, ASSL, 420, 199
Yan, L., et al. 2016, arXiv: 1611.02782
Yoshida, T., et al. 2014, AIPC, 1594, 284
Yuan, X., et al. 2013, IAUS, 288, 271

Appendix A

Dark Energy Camera on the Blanco 4-m telescope not only has the focal plane size, the 1970s 4 m-telescopes were built for, but also has good near infrared response. The goal of the DECamERON project[2] is a deep wide field high redshift photometric survey to study large scale structure and rare events. It reaches M* galaxies at redshift 6 at a wavelength of 1 micron, studying large scale structure and finding rare events. The aim is *not* to compete with deeper narrow surveys like BORG (Trenti et al. 2010). To maximise time allocation flexibility, all three of these DECam deep fields are circumpolar. Stacking of data is carried out by the DECam community pipeline (Valdes et al. 2014). Here, we report candidates for SNe at $Z = 4$ in the prime field. The light curves shown on the right are Z band. Pipeline stacks are archived in nine tiles of approximately 50 arcmin on a side. These tiles form a 3×3 matrix on the sky with tiles 1, 5, 9 as the main diagonal.

The postage stamps are Y band images. Images of the same epoch are aligned in columns. In Figures A1–A3, we see SNe that are bright in the first epoch, leaving only the host galaxy in the most recent epoch.

[2] http://astronomy.swin.edu.au/~jmould/decameron.htm

doi:10.1017/pasa.2017.6

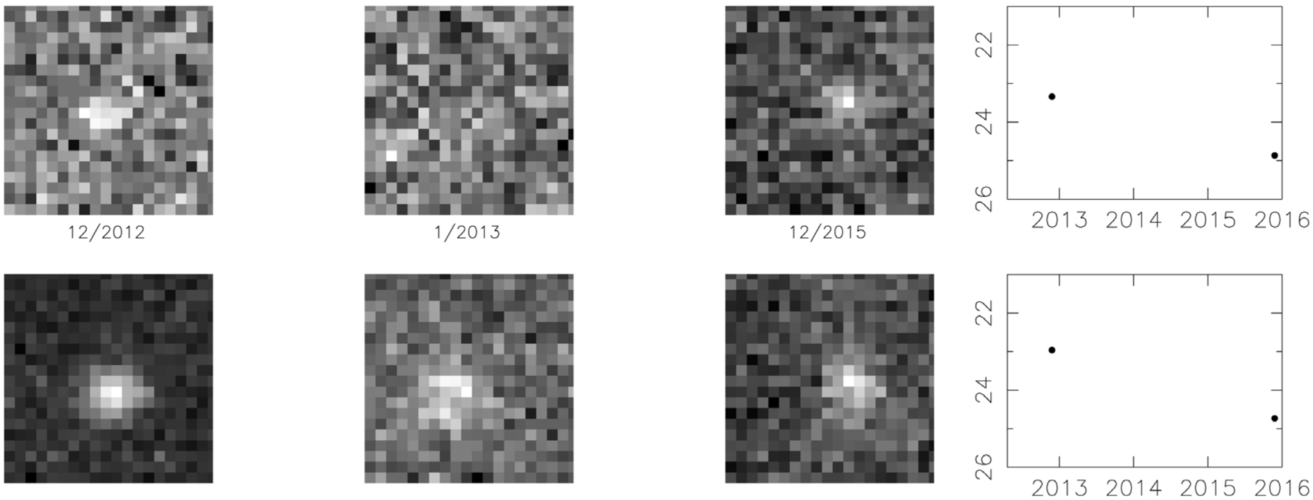

Figure A1. Tile 2 $Z = 4$ candidates.

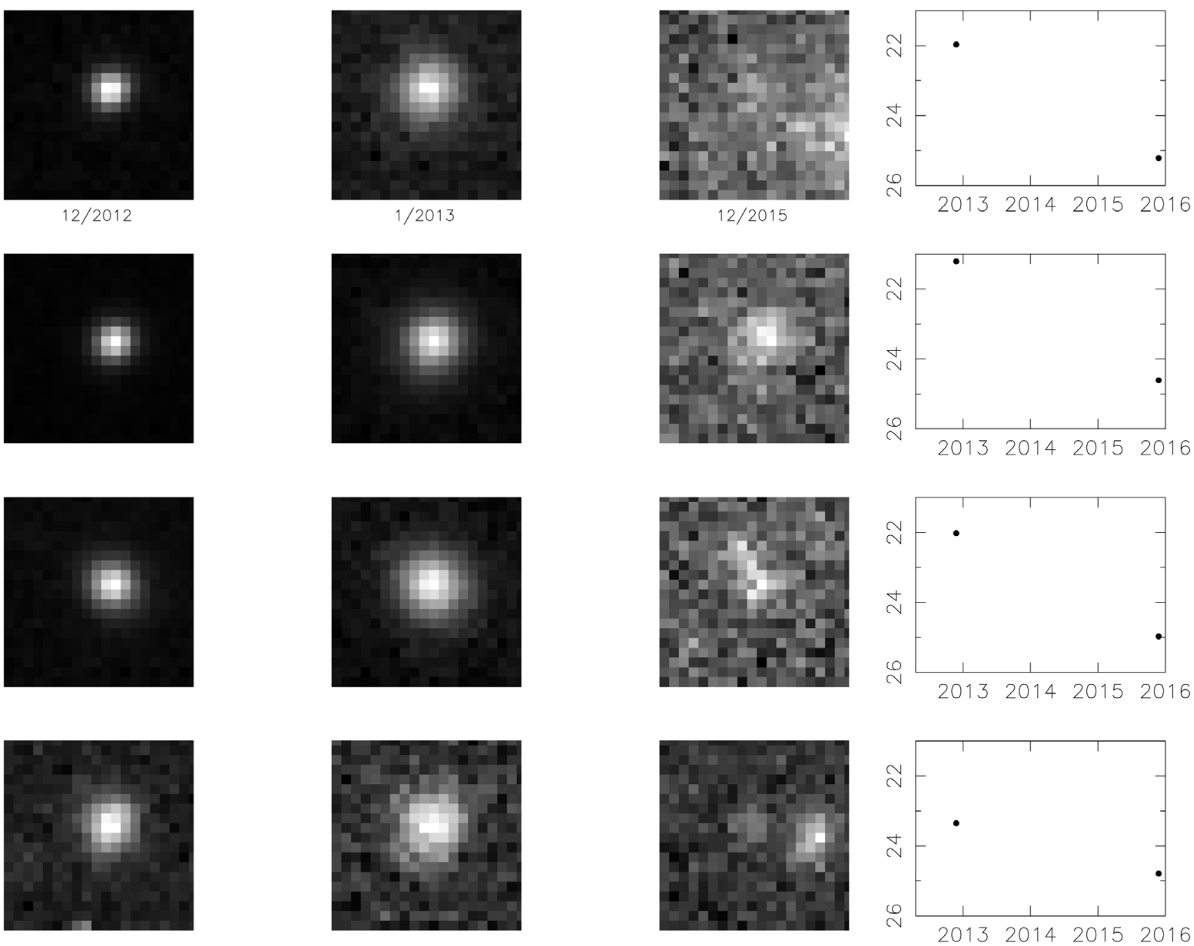

Figure A2. Tile 5 $Z = 4$ candidates.

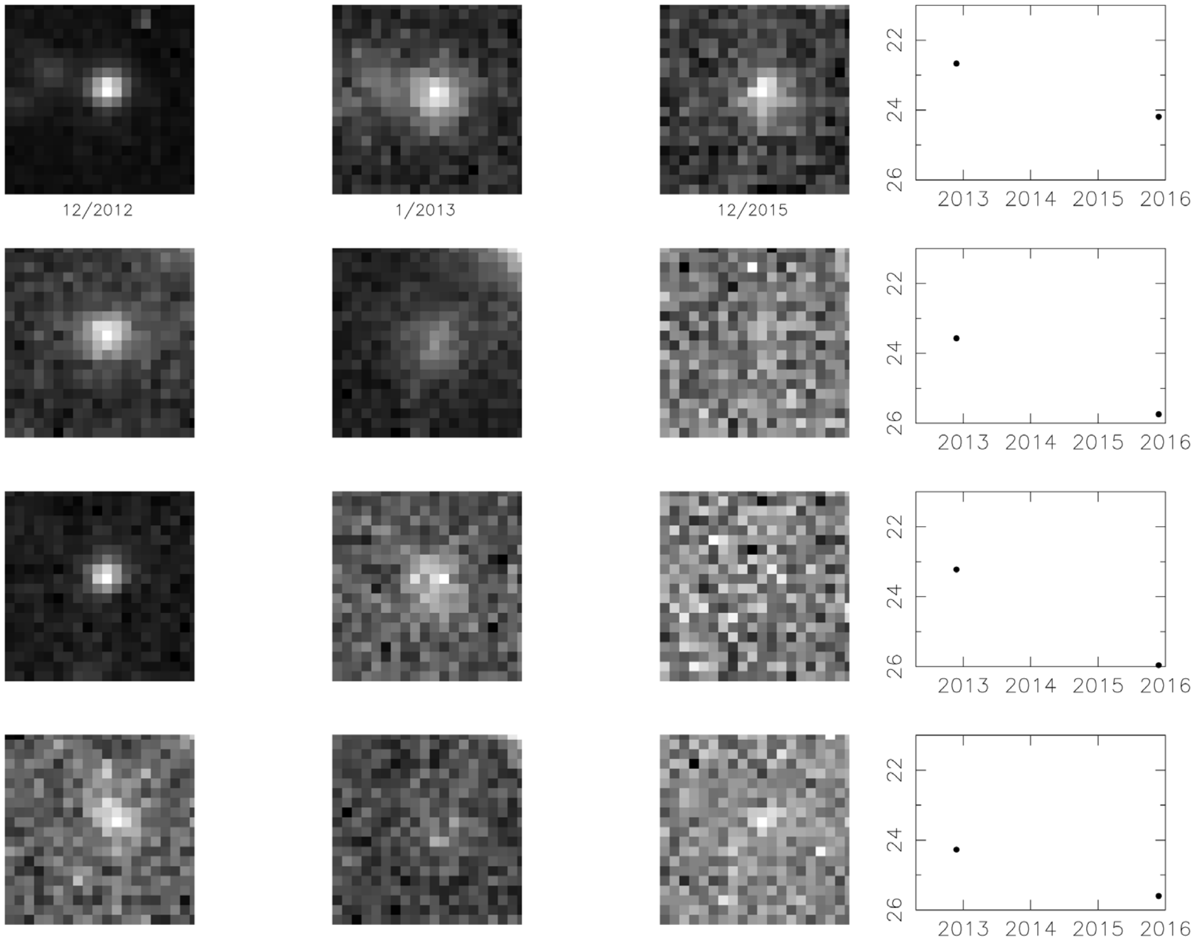

Figure A3. Tile 8 $Z = 4$ candidates.